I would like to thank my advisor Professor Gunnar Tufte for guiding me through my research in this exciting field and topic. In addition I would like to thank Johannes Høydahl Jensen, Vibeke Devold Valderhaug and Ola Huse Ramstad for helping and providing me with analytical tools and research data for this thesis.

Abstract

Technological advancement through the last century have made it possible to not only culture neurons in vitro (in glass outside the body), but also to a certain degree record and control their development. Micro-electrode array or Multi-electrode array (MEA, abbreviation for both) is one such technological advancement that allow for intra-cellular voltage spike recording and stimulation of cultured neurons. Through the electrodes mounted on the floor of the culturing chambers, spiking activities from the neurons can be captured, and stimuli can be passed to them through these bidirectional electrodes. In this thesis a customised random Boolean network (RBN) model have been made, to model the change in electrical activities of developing in vitro neural cultures.

Through the NTNU Cyborg initiative, MEAs with 60 electrodes is set up and available for experimentation. For this thesis, 4 neuron cultures were set up and recorded from initialisation and over a period of 18 days (only data from 15 days acquired). Due to the number and spatial placement of the electrodes, only a subset of the neuron culture activity is available through the recordings. Since the neurons tend to form clusters and connect to other clusters through their axon-pathways, we try to model this behaviour with our customised RBN model. In short the RBN is placed in a grid in the same fashion as the MEA. Furthermore a restriction is placed on the network, such that each node's chance of connecting to other nodes further away in the grid grows with time. We call the probabilities restricting each nodes connection possibilities the *distant connect* probabilities. These probabilities is governed by the parameter σ, where a $\sigma = 0$ only allows the nodes to connect to themselves, while greater values allows for connection to nodes further away.

Unfortunately no direct comparisons between the systems were done, due to issues with the neuron cultures. Complexity measures of the two systems could not be compared, since the data received from the cultures were not as representative as what have been observed in earlier successful cultures initiated. None of the 4 cultures initiated for this thesis reached a matured state before their formed clusters loosen up from the electrodes, and died out shortly after. However, experiments reveals that the complexity of the bit patterns produced by RBNs with our model approach can be controlled. 4 different intervals of σ was tested out with linear increase. The results shows a steady increase in complexity for all σ intervals, with the most complex patterns found at the end point of the largest interval.

Sammendrag

Teknologisk fremskritt gjennom det siste århundre har ikke bare gjort det mulig å dyrke nevroner in vitro(i glass utenfor kroppen), men også gjort det til en viss grad mulig å styre deres utvikling. Micro-electrode array eller Multi-electrode array (MEA, forkortelse for begge) er en slik teknologisk fremskritt, som gjør det mulig å ta opp intracellulær spenning, samt stimulere disse nevrokulturene. Gjennom elektroder festet på underlaget av kultiveringskamrene kan elektriske impulser fra nevronene bli fanget opp, og stimuli bli sendt sendt til dem gjennom disse bidireksjonale elektrodene. I denne oppgaven blir en egendefinert *tilfeldig Boolsk nettverk* (engelsk: random Boolean network, fork. RBN) modell brukt til å modellere aktiviteter av utviklende in vitro nevrokulturerer.

Gjennom NTNU Cyborg initiativet er MEAs med 60 elektroder satt opp og tilgjengelig for eksperimenter. For denne oppgaven ble det satt opp 4 nevrokulturer og deres aktivitet tatt opp i en periode over 18 dager (kun data fra 15 dager tilgjengelig). På grunn av antall og hvordan elektrodene er plassert i kammeret, blir ikke alt av nevroaktivitet tilgjengelig i opptakene. Siden nevroner har en tendens til å forme grupper og koble til andre grupper gjennom nervefibre, så prøver vi å modellere denne oppførselen med vår egendefinerte RBN modellen. I korte trekk er RBN modellen plassert i et rutenett på samme måte som MEA systemet. Videre har RBN modellen en restriksjon som gjør at sjansen hver node har til å koble til andre noder i nettverket øker med tiden. Vi kaller dette restriksjons-sannsynlighetssettet for *distant connect* sannsynlighten. Sannsynlighetene i dette *distant connect* settet er styrt av parameteren σ, hvor en $\sigma = 0$ tillater nodene kun muligheten til å koble til seg selv, mens større verdier for parameteret øker deres sjanse til å koble til andre noder lenger unna.

Uheldigvis ble ingen direkte sammenlikning mellom systemene gjort, på grunn av problemer med nevrokulturene. Kompleksitetsmålinger av disse to systemene kunne ikke sammenliknes, siden dataen fra kulturene ikke var representative sammenliknet med observasjoner fra tidligere suksessfulle kulturer. Ingen av de 4 kulturene som var satt opp nådde en moden fase, før deres formerte grupper løsnet fra elektrodene, og døde ut kort tid etter. Likevel viste kompleksitetsmålingene at bit-møstrene produsert av RBN'ene med våres oppsett kan kontrolleres. 4 ulike intervaller av σ var testet ut med linær økning. Resultatene viser en stabil økning av kompleksitet for alle intervaller av σ, med mest komplekse mønstre funnet i endepunktene av det største intervallet.

Preface

This report serves as the Master thesis for the author Cherdsak Mangmee. The report was written in the spring of 2018 at the Department of Computer Science(IDI) at the Norwegian University of Science and Technology(NTNU). The work was supervised by Professor Gunnar Tufte.

Table of Contents

Abstract i

Summary ii

Preface iii

Table of Contents vi

List of Tables vii

List of Figures xi

Thesis Structure xii

1 Introduction 1
- 1.1 Research Questions . . . 3

2 Background 5
- 2.1 Neurons . . . 5
- 2.2 Neuron Cultivation and Interfacing Systems . . . 6
  - 2.2.1 Multi-electrode Array . . . 7
  - 2.2.2 Neuron Activities in MEAs . . . 8
- 2.3 Random Boolean Network . . . 8
  - 2.3.1 Brief Overview . . . 8
  - 2.3.2 Characteristics of RBNs . . . 9

3 Methodology 13
- 3.1 Experimental Setup . . . 13
- 3.2 Neuron Raw Data Preparation . . . 13
- 3.3 RBN Model Setup . . . 14
  - 3.3.1 RBN Parameters . . . 14
  - 3.3.2 Execution Settings . . . 15

3.3.3 Connection Simulation and Spatial Placement of Nodes 16
3.3.4 Distant Connect 16
3.4 Pattern Comparison 18

4 Experiments **21**
4.1 Complexity Evolution of Spatially-Constrained RBNs 21
4.1.1 Description 21
4.1.2 Result 22
4.1.3 Discussion 23
4.2 Complexity Evolution of Neuron Cultures 28
4.2.1 Description 28
4.2.2 Result 28
4.2.3 Discussion 28
4.3 Complexity Comparison Between Neuron Spiking- and RBN Patterns . . 31
4.3.1 Discussion 31

5 Conclusion **33**
5.1 Conclusion 33
5.2 Future Work 34

Bibliography **35**

Appendix **37**
5.2.1 Distant Connect Probabilities 38

List of Tables

3.1 RBN Parameters 15

4.1 The ranges of σ values used to produce normal distributions for *distant connect* probabilities for the RBNs generated at each time step. All ranges have a linear increase between 0 and the maximum σ value. 22
4.2 End point probabilities of the different configurations tested. The leftover values at the long tails are removed and the probabilities normalised to 1. 27

5.1 Distant connect probabilities at each time step with σ in range [0,3], where the first index corresponds to the chance of connecting to itself. The last index is the leftover probabilities in the long tails on both sides of the curve. 38
5.2 Distant connect probabilities at each time step with σ in range [0,4], where the first index corresponds to the chance of connecting to itself. The last index is the leftover probabilities in the long tails on both sides of the curve. 39
5.3 Distant connect probabilities at each time step with σ in range [0,5], where the first index corresponds to the chance of connecting to itself. The last index is the leftover probabilities in the long tails on both sides of the curve. 39
5.4 Distant connect probabilities at each time step with σ in range [0,6], where the first index corresponds to the chance of connecting to itself. The last index is the leftover probabilities in the long tails on both sides of the curve. 40

List of Figures

1.1 Evolution of cultivated neuron cultures in petri dishes with electrodes. D,E and F shows evolution from early, semi-developed and matured stage (black dots are electrodes). The D1, E1 and F1 reflects D, E and F and shows how spiking activity might look like in a single electrode from the different stages. Illustration from [14] 2

1.2 Example of a mimicked RBN system with nodes aligned in the same fashion as the MEA recording framework from the neuro-science department(INB) at NTNU. From upper left to lower right, the evolution of how connections changes as the nodes of the RBN are gradually allowed to connect to other nodes further and further away. Note: The RBNs shown are 4 different networks all generated by different probabilities of connection allowance. 3

2.1 Illustration of neuron anatomy by BruceBlaus via Wikipedia Commons . 6

2.2 Timeline of the emergence of methods for culturing neurons, since the first findings of Harrison in 1910. Illustration from [12]. 6

2.3 Micro-electrode array/multi-electrode array (MEA), a system that allows long-term observation, perturbation and readout from neuron cultures. Photo: Kai T. Dragland 7

2.4 Electrodes in an incubation chamber. In this particular example, there are a total of 60 bidirectional electrodes that can both stimulate and record neurons and their activities. 8

2.5 Example of function evaluation of a node. The value of neighbouring states are arguments for the evaluation function for each node. In this example the evaluation function is an logic AND function. 9

2.6 Illustration of point and cycle attractors and their attractor basin. 10

2.7 A comparison between networks in the three different categories ordered, critical and chaotic. States of nodes plotted horizontally, time flows downwards. 11

3.1
Left: Attractor-measurement test of RBNs with $N = 20$ and K in the range [1-6], where all possible 2^{2^k} transition functions are allowed. For each K, 1000 candidate networks were generated and executed with one random initial state with equal amount of 0s and 1s.
Right: Attractor-measurement test where N is in the range [10-20] and $K = 2$. All possible 2^{2^k} transition functions are allowed. For each N, 1000 candidate networks were generated and executed with one random initial state with equal amount of 0s and 1s. 14

3.2 The first illustration shows how the transient states of RBN systems that does not reach an attractor are glued together as a bit-string. The second illustration shows how RBN systems that does reach an attractor are glued together as a bit-string. 15

3.3 Each coloured region represents the chance a node have to connect to its neighbours. The middle portion centred on the mean is the chance of connecting to the node itself (distance 1). The other colours represents the chance of connecting to nodes with distance 2,3...8 away. The normal curve displayed have $\mu = 0$ and $\sigma = 1$. 17

3.4 Example of how a node's neighbours by distance can look like. In this illustration the current node is highlighted in red and its maximum neighbour distance is 5, where connection to itself counts as distance: 1. For some nodes, e.g. those in the corners, the maximum neighbour distance is 8. 17

3.5 Spatial node layout of the MEA system 18

3.6 Overview of the comparison process.
Left: The neuron culture outputs data to the electrodes, the data gets processed and turned into bit string for comparison.
Right: The RBNs generated represents virtual nodes from a larger system, mimicking the electrodes and outputs bit string for comparison. 19

4.1 The normal distribution function used to generate each probability value for each time step for the different configurations. μ = 0 and σ is in the range shown in table 4.1. 21

4.2
Kolmogorov complexity evolution over 15 discrete time steps with linear increase of the *distant connect* parameter σ. Four different ranges of σ is shown. Each time step consists of 1000 individual RBNs generated with the probability distribution adjusted by σ. 23

4.3 One candidate RBN from time step 0, 5, 10 and 14 with the σ : [0,3]. From upper left to lower right, the evolution of how connections changes as the nodes of the RBN are gradually allowed to connect to other nodes further and further away. Note: All RBNs are generated at random with *distant connect* probabilities of each respective σ values in the range [0,3], not the same network. 24

4.4 One candidate RBN from time step 0, 5, 10 and 14 with the σ : [0,6]. From upper left to lower right, the evolution of how connections changes as the nodes of the RBN are gradually allowed to connect to other nodes further and further away. Note: All RBNs are generated at random with *distant connect* probabilities of each respective σ values in the range [0,6], not the same network. 25
4.5 Mean values from fig 4.2 plotted against each other. 26
4.6 All plots from 4.2 together with the whole range of complexity values (not zoomed in). 26
4.7 Spike count of the RBN configuration with the σ range [0,3].The maximum spikes that can occur per sample is $59 \times 20,000$ = 1,180,000. 27
4.8 Kolmogorov complexity for the neuron cultures labelled 33, 34, 36 and 37. The data stream from each day is sampled 1000 times, with a data sample window of 20, 000 in length. The start time for each sample is picked at random and fixed across all 59 channels. 29
4.9 Spike count for the neuron cultures labelled 33, 34, 36 and 37. The sample set of data is the same as the ones used in figure 4.8. Data stream from each day is sampled 1000 times, with a data sample window of 20,000 in length for each channel. The start time for each sample is picked at random and fixed across all 59 channels. Note: last day of culture 36 is missing due to technical problems with the recordings. 30
4.10 Mean value of spike count and Kolmogorov complexity from the figures 4.8 and 4.9. 30
4.11 Approximated Kolmogorov complexity of the firing patterns over a one year period.[14] Note scaling difference between this and the plots from the experiments of this thesis. 31

Thesis Structure

This thesis is structured as follows:

Chapter 1 introduces the reader to the topic of the thesis.
Chapter 2 provides background information on multi-electrode array (MEA) and random Boolean networks. Where the first is a technology that allows stimulation and readout of cultured neuron cultures, and the second is a model that have been customised and used to model the electrodes of the MEA.
Chapter 3 provides information about the experimental setup and methodologies used to perform the experiments.
Chapter 4 describes the experiments, results and discusses about them.
Chapter 5 concludes the thesis and gives a brief explanation of potential future work.

Chapter 1

Introduction

Ever since the landmark finding by Ross Granville Harrison in 1910 – that neurons can be cultured outside the body – different methods/techniques for neuron culturing have emerged as the technology have advanced[12]. These techniques gave the possibility for simulation of in vivo(within the living) micro-environment of cells to be done in glass chambers outside the body, in vitro(within the glass) that is. Being able to do so is quite convenient and often a critical prerequisite for studying neuron cells. The technique in focus for this thesis is the multi-electrode array(MEA), which is a non-invasive electrophysiology laboratory technique. With this technique an array of planar electrodes can be used to record and/or stimulate cultured neuron cells in petri dish-like chambers. Through the NTNU Cyborg initiative, neuron cultures have been successfully kept alive for a period of over a year in these chambers[14]. With such a test bench up and running, new cultures can be set up for research. One interesting and observable characteristic of neurons is that they tend to form clusters and create axon pathways in between. As the cultures mature, these connections have been observed to reach out to other quite distant groups of neurons. This characteristic or self-organisation property of neurons is still not well understood. Observing how neurons with random spatial placements moves and turns into clusters with highway-like paths between them is in itself fascinating(see 1.1).

As an attempt to model this self-organisation phenomena neurons have, random Boolean network (RBN[3]) was proposed. This model was famously used by Stuart Kauffman as a model for genetic regulatory networks[6]. The model is quite useful as abstraction for many physical systems. In short RBNs consists of a set of nodes and edges connecting them together. For each clock time (depending on the updating scheme) each node's Boolean value will be updated by values propagated from other nodes connecting to itself (see chapter 2.3). Since there are approximately 20,000 - 100,000 neurons in the incubation chamber and only 60 static electrodes, the electrodes can be viewed as an abstraction of the neurons in the chamber. Pin pricks into the neuron culture. As the culture evolves, clusters might be formed on top of the electrodes and their activities captured by the instrument. Illustration of this evolution can be seen in figure 1.1. This change of activity is

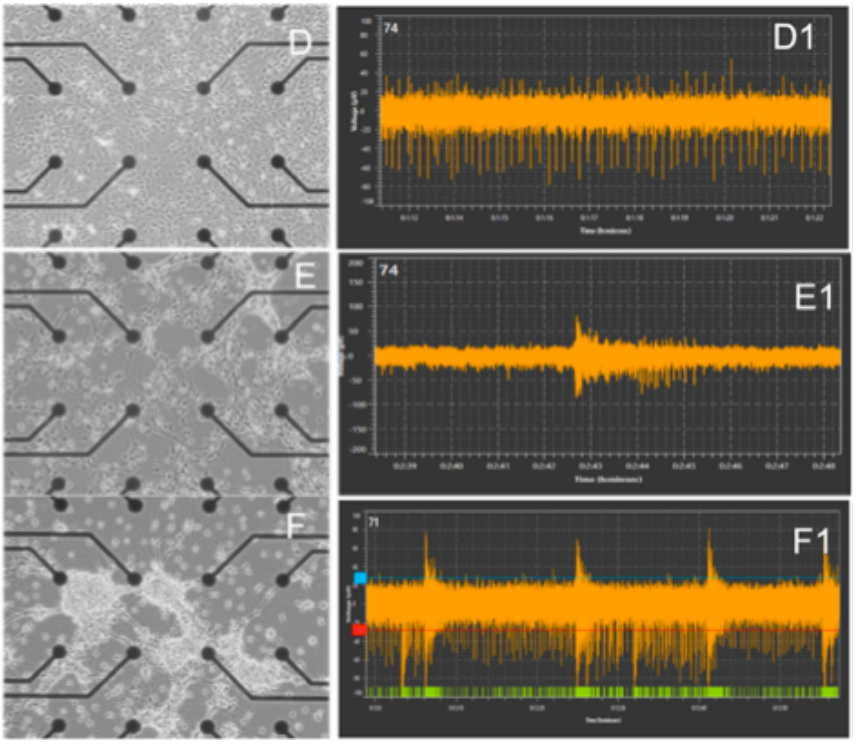

Figure 1.1: Evolution of cultivated neuron cultures in petri dishes with electrodes. D,E and F shows evolution from early, semi-developed and matured stage (black dots are electrodes). The D1, E1 and F1 reflects D, E and F and shows how spiking activity might look like in a single electrode from the different stages. Illustration from [14]

quite interesting in that they seem to be related to the change in the neuron structures. Similarly, the nodes of a RBN can be placed on a grid in the same manner, and the connection between them act as axon pathways between neuron-clustered electrodes in the incubation chamber. The idea is to try as a first step to compare patterns created by these specialised RBNs with the signal patterns of the neuron cultures, by gradually allowing the nodes to connect to other nodes further away. As time goes the nodes of RBNs generated will have an increase in their chance of connecting to nodes further away. By changing this connection governing probability called *distant connect*, changes will occur both in the RBNs structure and patterns produced by them. The analysis of this might provide insight on how change in structure affects the signal patterns of the neuron cultures. An example of how the RBNs can look like in different phases is shown in figure 1.2.

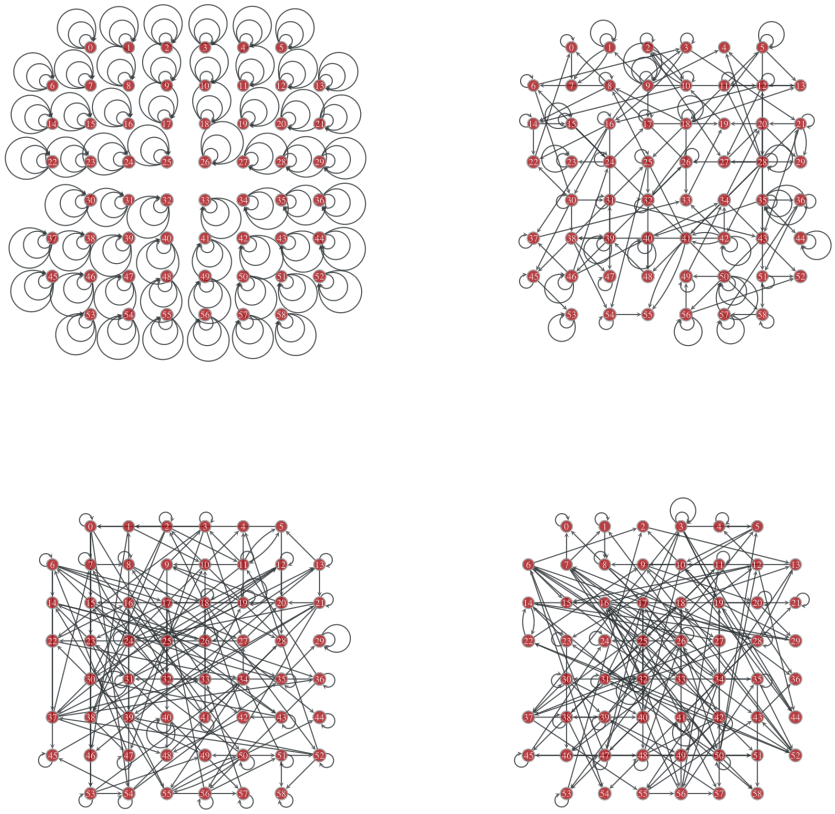

Figure 1.2: Example of a mimicked RBN system with nodes aligned in the same fashion as the MEA recording framework from the neuro-science department(INB) at NTNU. From upper left to lower right, the evolution of how connections changes as the nodes of the RBN are gradually allowed to connect to other nodes further and further away. Note: The RBNs shown are 4 different networks all generated by different probabilities of connection allowance.

1.1 Research Questions

There are two main questions that will be investigated in this thesis:

- Is it possible to control the complexity evolution of spatially-constrained RBNs by restricting their connection possibilities?
- Can RBNs be modelled to yield similar pattern complexity as neuron cultures?

Chapter 2

Background

2.1 Neurons

Neurons are the main building blocks of the brain. These specialised cells can grow into different shapes over time and form connections to other neurons and cell types such as receptors(stimuli to impulse) and effectors(impulse to action). As single units, neurons receives signals through its dendrites, processes the signal through its cell body and propagates the signal further through its axon to other neurons or cell types. An illustration of the neuron anatomy can be seen in figure 2.1. It does not require many neurons to make an organism able to take in information from the environment and respond to that information. Only 302 neurons are needed for a hermaphrodite nematode worm to sustain such a process[17]. However, the neurons alone are not sufficient without the correct types of connections between them. Although the number of neurons are quite few in these worms, research have shown very complex inter-connectivity in them[17]. This makes the human brain, which contains about 86 billion neurons[5] very hard to study. Not only does these neurons enable us to take in information from the environment and respond to it, but it also sustains and regulate different body parts and give us the ability to reason.

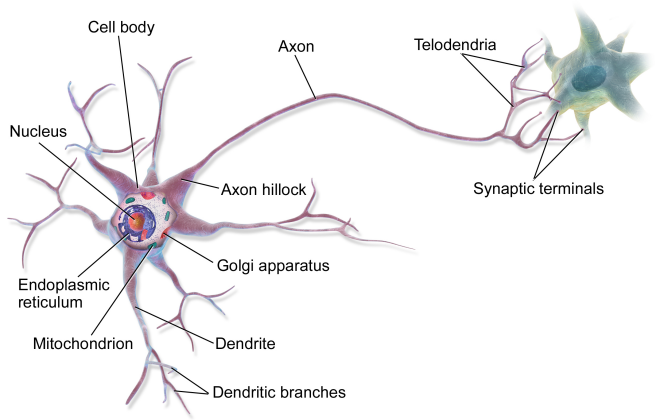

Figure 2.1: Illustration of neuron anatomy by BruceBlaus via Wikipedia Commons

2.2 Neuron Cultivation and Interfacing Systems

Through the last century, different types of cultivation methods have been used to study the nature of neurons. Starting with the hanging drop method conducted by Ross Harrison in 1910, where he for the first time made direct observation of living cells in vitro possible[12] to present micro-environment techniques, researchers can now not only observe but also to a certain degree control neuron development. Illustration of this emergence of methods for culturing neurons can be seen in 2.2, and a well written summary of this can be read in [12].

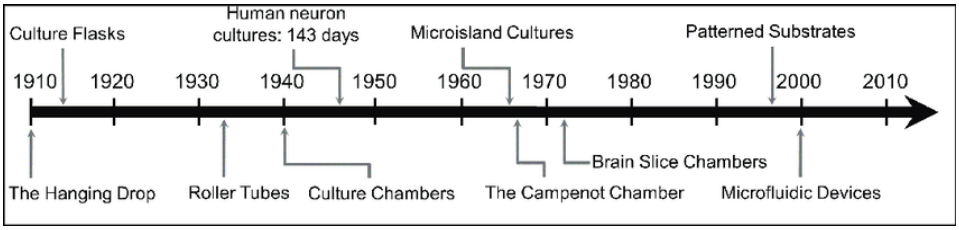

Figure 2.2: Timeline of the emergence of methods for culturing neurons, since the first findings of Harrison in 1910. Illustration from [12].

With technological advancement, neurons can now be cultured in incubation chambers that can mimic the biological environment in which they usually lives. In these chambers temperature, humidity and gas levels are regulated close to what it is in the body. Furthermore, conventional medium containing nutrients, growth hormones and antibiotics are added to sustain the cells needs. With such chambers, the neurons can be kept alive for extended period of time (e.g. in the Socrates project by NTNU [14]), making it possible to repeatedly observe development without risk of infection from bacteria. Aside from being able to keep neuron cultures healthy and alive, there are also some systems that

allow perturbations and readouts from the culture, such as micro-electrode arrays/multi-electrode arrays (MEAs, abbreviation for both), illustration in 2.3. Hardware systems as such gives the possibility to analyse neuron activity in the chambers by recordings through the electrodes that can capture intra-cellular electrical signals. They enable long-term monitoring of electrophysiological activities among neurons cells in the cultures, providing the possibility of observing spatio-temporal patterns of activities between neurons in a two dimensional layer.

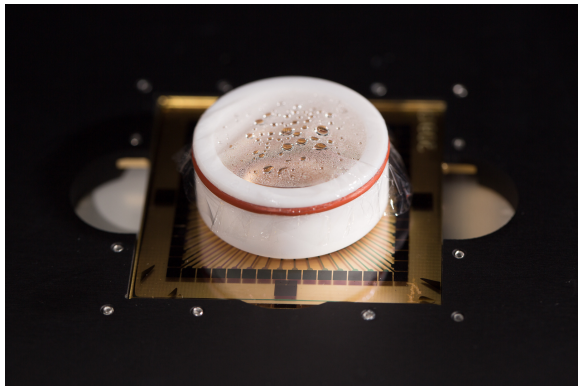

Figure 2.3: Micro-electrode array/multi-electrode array (MEA), a system that allows long-term observation, perturbation and readout from neuron cultures. Photo: Kai T. Dragland

2.2.1 Multi-electrode Array

Multi-electrode arrays(MEAs) are specialised devices often made by photo-lithographic techniques from the semiconductor industry[20]. These are specialised chambers in which living neurons can be grown onto. The floor surface of the chambers are equipped with bidirectional electrodes that can be used to stimulate and record neurons and their activities. An illustration of these electrodes can be seen in figure 2.4. The activity of spatially close neurons can be captured by the electrodes. Furthermore the electrodes can pass electrical voltages (not harmful for the cells) to stimulate neurons close by. For the NTNU Cyborg project, the MEA2100-60-system from MultiChannel Systems[13] is used for the recording at present time. The number of electrodes in this system is 60 (with one being ground/reference node). This is very far from covering every single cells, since there usually are tens to hundreds of thousands cells in the cultivation chamber. Ideally the activity of each cell should be captured for a complete analysis of the system as a whole, something that might be possible in the years to come. In fact research are being conducted where the electrode numbers have been greatly increased, for instance Ballini et al.[10] with 1024-channel experiments and CMOS MEA with 26,400 electrodes. Although only a small subspace of the whole chamber is reachable in terms of readout and stimuli, it is still useful to capture activities given that the neurons grows on top of the electrodes.

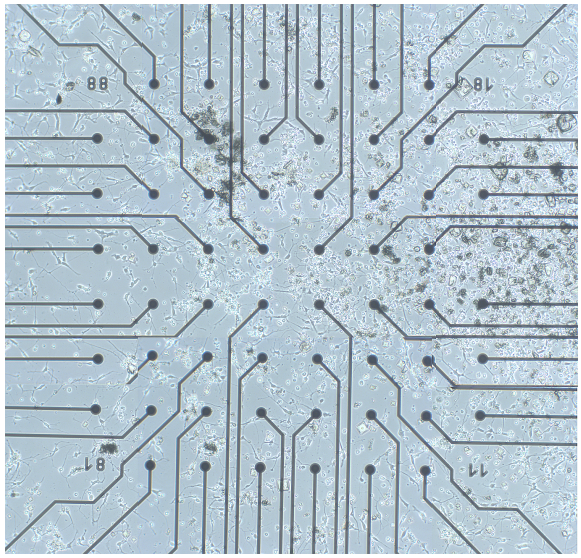

Figure 2.4: Electrodes in an incubation chamber. In this particular example, there are a total of 60 bidirectional electrodes that can both stimulate and record neurons and their activities.

2.2.2 Neuron Activities in MEAs

Observations through neuron interfacing systems have shown that neuron cultures tend to develop some sort of synchronous and spontaneous bursting activities when they mature[2]. Research conducted by DeMarse et. al[19] have shown that consistent bursting activity is likely to dominate after 18-25 days for in-vitro cultures. In the same study, it was also reported spiking burst to be semi-periodic and occurring every 5-15 seconds, typically 100 to 1000 ms in duration. Furthermore, the study shows the activity to be network wide burst rather than being eliciting responses between few neurons. Although the behaviour of such bursting activity is not completely understood, suggestions have been that the cultures might lack neurons in order to be stable[4]. It might as well be due to the fact that the neurons are placed in glass chambers and not in their natural environment[2]. However, these observations helps greatly in pin pointing what can be expected when looking at the data generated by the cultivated neurons.

2.3 Random Boolean Network

2.3.1 Brief Overview

Random Boolean networks (RBN) are discrete dynamical systems, originally proposed by Stuart Kauffman in 1969. They are also known as N-K models or Kauffman networks. The model in its proposal, was used as a simple model for gene regulatory networks [6], the complex types of networks that regulates how genes in living cells interact with each other. In its simplest form, RBNs consists of N nodes and M links (edges) between the

nodes. Each node *i* can take two different states, usually $s_i \in \{0, 1\}$. The number of links into each node *i* (in-degree) is denoted by k_i and is chosen randomly from the distribution $P(k_i)$. The dynamics of the network is governed by a set of Boolean transition functions. At each time step, the next state value of each node is obtained by evaluating the node's transition function. The arguments for this function is the current value of its neighbouring nodes, propagating from the edges. An illustration of the function evaluation process is shown in figure 2.5. The set of transition functions allowed for each node can be restricted, but is often chosen to be all possible 2^{2^k} functions, where *k* is the number in-degree to the node. Cellular automata's are special cases of random Boolean networks where the cells are arranged in the form of a regular mesh of any dimension and the average connectivity k is the same for all the cells of the network. Wolfram elementary cellular automata[18] and Conway's Game of Life[11] are perhaps two of the more well known network configurations that have been researched in the last several decades.

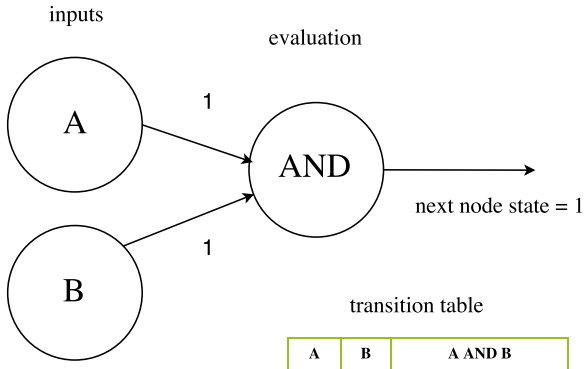

transition table

A	B	A AND B
0	0	0
0	1	0
1	0	0
1	1	1

Figure 2.5: Example of function evaluation of a node. The value of neighbouring states are arguments for the evaluation function for each node. In this example the evaluation function is an logic AND function.

2.3.2 Characteristics of RBNs

In the classical model, the updating scheme of the network is *synchronous*, meaning that all nodes at time $t + 1$ depend on the states of all nodes at time t. The state space of these RBNs are finite with a total of 2^N states, where N is the number of nodes in the network. As the states of a RBN is finite, the system will eventually revisit the same state. When such an event happens, the system have reached an *attractor* and will oscillate in this *loop* for the rest of its run time. The attractor can be divided into two groups: *point*

attractor (single-state oscillation) and *cycle* attractor (multi-state oscillation). The set of states that flows towards an attractor is called the attractor *basin*[3]. An illustration of this is shown in figure 2.6. Apart from the classical model, there exist other classes of RBNs. By changing the updating scheme to asynchronous or partly asynchronous, the system can become non-deterministic. Furthermore the dynamics of RBN's phases can be categorised as ordered, critical or chaotic. These categories divides the networks by their ability to change over time. This helps determine whether similar states in the network converge or diverge over time, and also the network's robustness to perturbations from outside. There are different methods of measuring the stability of the network e.g. by looking at the network's "sensitivity to initial conditions", "damage spreading" and "robustness to perturbations"[3]. A node can be "mutated", "damaged" or "perturb" by having its state flipped. Generally RBNs in critical phases are the most interesting ones. These seems to support information transmission, storage and modification, the capabilities that are required for computation[8]. Critical networks are found at the so called "edge of chaos", the transition between ordered and chaos[3]. Usually networks of such nature can be found with an in-degree k averaged on around 2, although it is possible to find them for other values too. To visually observe the state space of the different phases of the network one can plot the network's state progression in a lattice, an illustration is shown in figure 2.7.

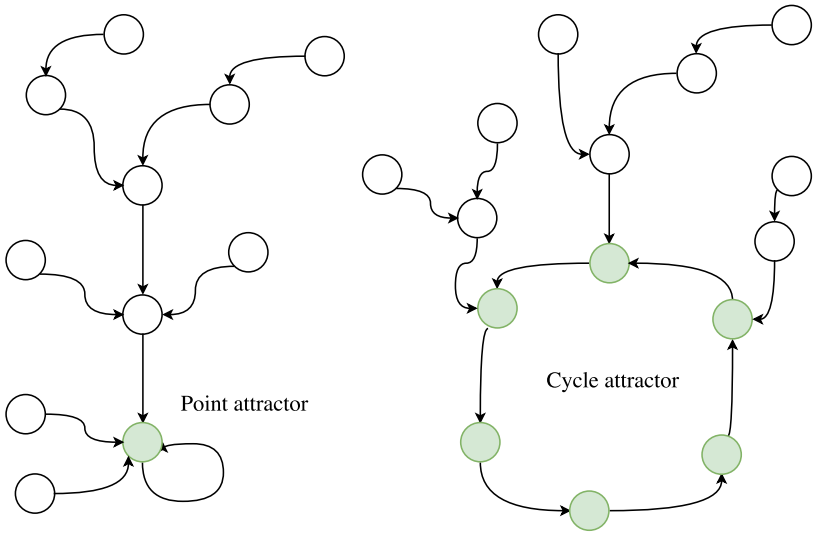

Figure 2.6: Illustration of point and cycle attractors and their attractor basin.

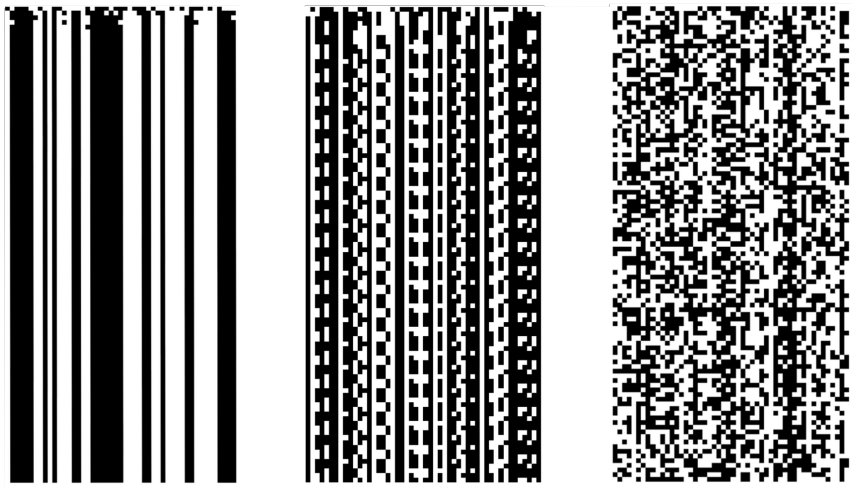

a) Ordered Phase K=1 b) Critical phase K=2 c) Chaotic phase K>2

Figure 2.7: A comparison between networks in the three different categories ordered, critical and chaotic. States of nodes plotted horizontally, time flows downwards.

Chapter 3

Methodology

3.1 Experimental Setup

The experimental setup used for this thesis consists of three main components. These include, data preparation, network model construction & execution and complexity comparison. The first part is a data preparation component. This is where raw data from the neuron recordings will be turned into string of bits through spike filtering. The second part will consist of RBN construction and execution. In this part, RBN configuration are chosen as a model to produce data for comparison. For the last part, the filtered data from neuron recordings are compared to the data produced by the RBN configurations. Two different comparison methods will be used namely Kolmogorov complexity[9] and spike counting.

3.2 Neuron Raw Data Preparation

The data acquired for this thesis is generated by the MEA2100-60-System [13], seeded with iPSC-Derived Neural Stem Cells (description in 5.2). The procedure was executed by the Department of Neuromedicine and Movement Science (INB) at NTNU. The data from the recordings comes in streams for each channels. For this particular system, there are in all 59 record-able channels. Depending on where the cultivated neurons form clusters, the activities recorded might vary from culture to culture. Sometime cultures can give good readouts from multiple electrodes, while other it might give a few or none. Since the aim is to capture the overall activity of the neuron cultures the same filter is applied across all channel. This means that the channels with little to no activities will end up giving zero patterns. The filter is simply a threshold function that accepts every value exceeding the threshold value (negative or positive). The data that comes from the recording has a sample rate of 10 kHz(10,000 samples per second) and the recordings are done over a period of around 10 minutes per day. To keep the process simple, only 2 seconds of the each recording is used (multiple samples), since neurons produce repeatable firing

patterns. This makes a bitstring of the length of 20,000 for each channel of the recording system.

3.3 RBN Model Setup

3.3.1 RBN Parameters

As the search space is quite large per combination of RBN, it is usually not possible to capture the whole dynamic of a network. The number of different N-K combination alone is as large as $(\frac{(2^{2^K} N!)}{(N-K)!})^N$ [3]. Therefore the size chosen for N and K is 59 and 3, with N being the same number as active electrodes in the neuron culture recording instruments. The number of K is 3 because it can often produce patterns resembling a system that is at the edge of chaos. Although K = 2 is usually what have been the standard for systems in that phase [1], it was chosen to be 3 for this experiments due to connection constraints applied to these RBNs . Furthermore, a couple of attractor-measurement tests were conducted to verify the nature of attractor lengths for different values of K for RBNs with 20 nodes, and another with $K = 2$ and N in the range between 10-20 (see 3.1). By observation, it seems like a value of $K > 2$ would yield more interesting and varied dynamics than for $K = 2$. Finally one initial state is used to keep the testing framework simple and restrict the search space. The initial state is a bitstring of repeating ”01” with a length of N. The parameters are summarised in table 3.1.

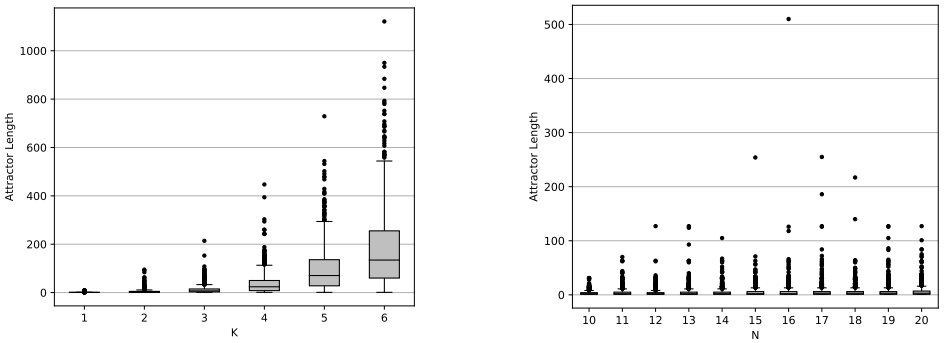

Figure 3.1:
Left: Attractor-measurement test of RBNs with $N = 20$ and K in the range [1-6], where all possible 2^{2^k} transition functions are allowed. For each K, 1000 candidate networks were generated and executed with one random initial state with equal amount of 0s and 1s.
Right: Attractor-measurement test where N is in the range [10-20] and $K = 2$. All possible 2^{2^k} transition functions are allowed. For each N, 1000 candidate networks were generated and executed with one random initial state with equal amount of 0s and 1s.

Table 3.1: RBN Parameters

Parameter	Configuration
Nodes N	59
In-degree K	3
Updating scheme	Synchronous
Execution time steps	20000
Initial state	0101010101010101010101...10
Transition functions	all 2^{2^k} functions

3.3.2 Execution Settings

The RBNs are running with a maximum of 20,000 time steps to match the sample size chosen for the neuron spiking data. Note that all RBNs are homogeneous in connectivity (all have the same number of in-degree) and that the connectivity stay the same for its entire run time. For RBN systems that does not reach an attractor, their movement through the state space are returned and glued together as a bit-string. For the other RBN systems that does reach an attractor, their transient states are glued together with the repeated attractor loop for the remaining time steps. Patterns returned are of the same size, 59×20000 that is. An illustration of this bit-string creation is shown in 3.2.

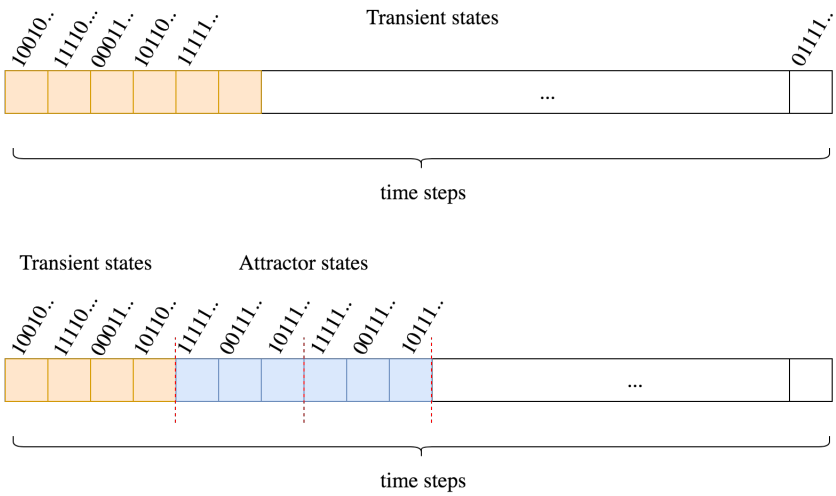

Figure 3.2: The first illustration shows how the transient states of RBN systems that does not reach an attractor are glued together as a bit-string. The second illustration shows how RBN systems that does reach an attractor are glued together as a bit-string.

3.3.3 Connection Simulation and Spatial Placement of Nodes

As neurons grows over time, their axons can be wired to other quite distant neurons or cells (e.g. the lengthy axons from the spinal cord to the big toes). Neurons in cultivation chambers is therefore assumed to be able to reach out to any other neurons in the chamber, considering that the surface area is less than 49×49 mm in size. However through visual observations, the neurons seem to have a good chance of connecting to other neurons close by upon initialisation and form clusters. It was therefore proposed to add a constraint onto the RBN, to simulate the impulses from these clusters through the electrodes. This constraint is called *distant-connect* and represents the chance a node have to connect to its neighbours. The chance of connecting to distant neighbours is initially zero, meaning that each node will only connect to itself and its closest neighbours early on in the process. As the time goes, the networks generated will have greater chances of connecting to more distant nodes. The distance between two nodes is the shortest distance where horizontal, vertical and diagonal jumps are allowed. Chosen spatial placement of the nodes are the same as for the MEA-grid layout to mimic the system. Illustration of this can be reviewed in figure 3.5. Furthermore, an example of different distances for a given node is shown in figure 3.4.

3.3.4 Distant Connect

The *distant connect* constraint is a list of probabilities a node have to connect to other nodes of all distances available. For instance the *distant connect* probabilities [0.8, 0.2, 0, 0, 0, 0, 0, 0] means that the chance a node have to connect to itself is 80% (distance 1) and 20% to any of its closest neighbours (distance 2). This list of probability constraint is governed by the normal probability distribution $N(\mu, \sigma^2)$ centred on zero ($\mu = 0$). Each standard deviation interval from the mean represents the chance a node have to connect to its neighbours. The interval from 0 to 1 and 0 to -1 (both sides of the curve), represents the chance a node have to connect to itself (distance 1). The interval from 1 to 2 and -1 to -2 represents the chance of connecting to its closest neighbours (distance 2), and so on. An illustration is shown in figure 3.3. For nodes that does not have possible neighbours of all distances (e.g. those in the middle of the grid), the probabilities of available distances are normalised. For instance, if the maximum distance within a node's reach is 3, the *distant connect* probabilities [0.6, 0.2, 0.1, 0.1, 0, 0, 0, 0] will be turned into [0.6666, 0.2222, 0.1111]. By increasing the standard deviation σ, the curve will flatten out further away from the mean and the tail on both side reach zero further out. For σ value close to zero, the probabilities will lump around the mean, restricting the node's probability to connect to no other than itself. Letting the σ slowly increase, the RBNs generated will have an increase in each node's chance of connect to other nodes further away.

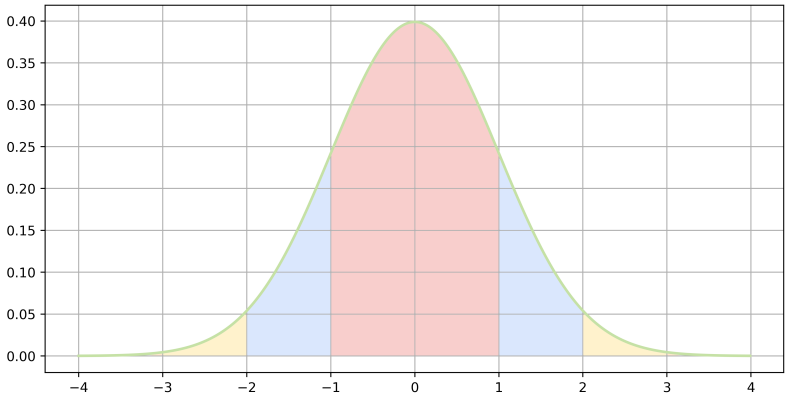

Figure 3.3: Each coloured region represents the chance a node have to connect to its neighbours. The middle portion centred on the mean is the chance of connecting to the node itself (distance 1). The other colours represents the chance of connecting to nodes with distance 2,3...8 away. The normal curve displayed have $\mu = 0$ and $\sigma = 1$.

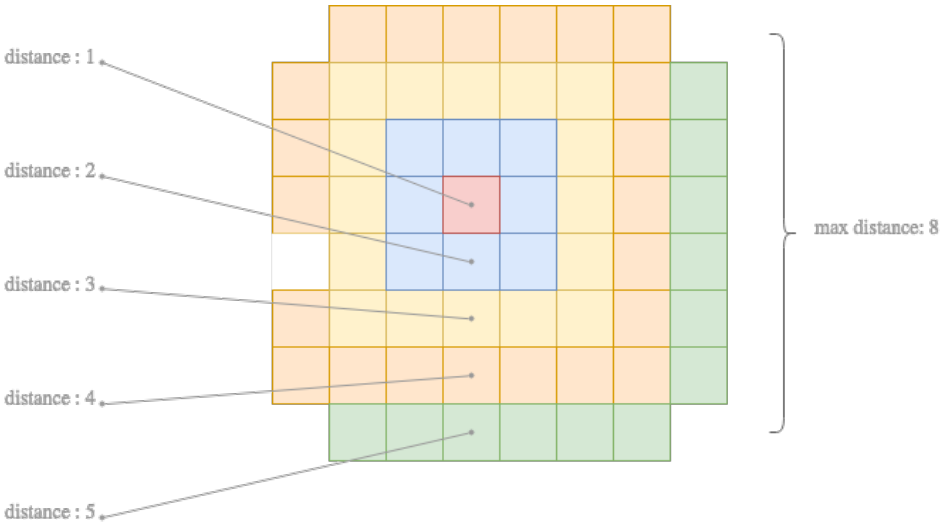

Figure 3.4: Example of how a node's neighbours by distance can look like. In this illustration the current node is highlighted in red and its maximum neighbour distance is 5, where connection to itself counts as distance: 1. For some nodes, e.g. those in the corners, the maximum neighbour distance is 8.

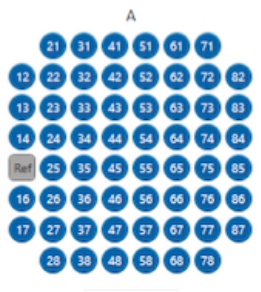

Figure 3.5: Spatial node layout of the MEA system

3.4 Pattern Comparison

Due to many yet unknown mechanisms about neurons and the brain, it is difficult to set any general comparison properties. One way to look at the systems is to view them as two black boxes that produces data patterns as time goes. Figure 3.6 shows the overview of this comparison process, where both systems gets reduced to string of bits. A classic way to compare string of bits and their complexity is by using compressors also known as zipping. When one zip a file, the compressor's algorithm does its best to turn the given data into something smaller in size without losing information. By generating symbols out of patterns that are identical, the compressor can reduce the file size substantially. More complex patterns yields more unique symbols and thus less compression. The catch is that, more pattern complexity makes the .zip file bigger and the opposite when the patterns are more repeatable. This type of complexity is called Kolmogorov complexity[9] and used as the main comparison property for the experiments. Although no perfect compression algorithm exists, it is still a good approximation to the bigger picture. The compression algorithm used for this task is the Bzip2 algorithm [15].

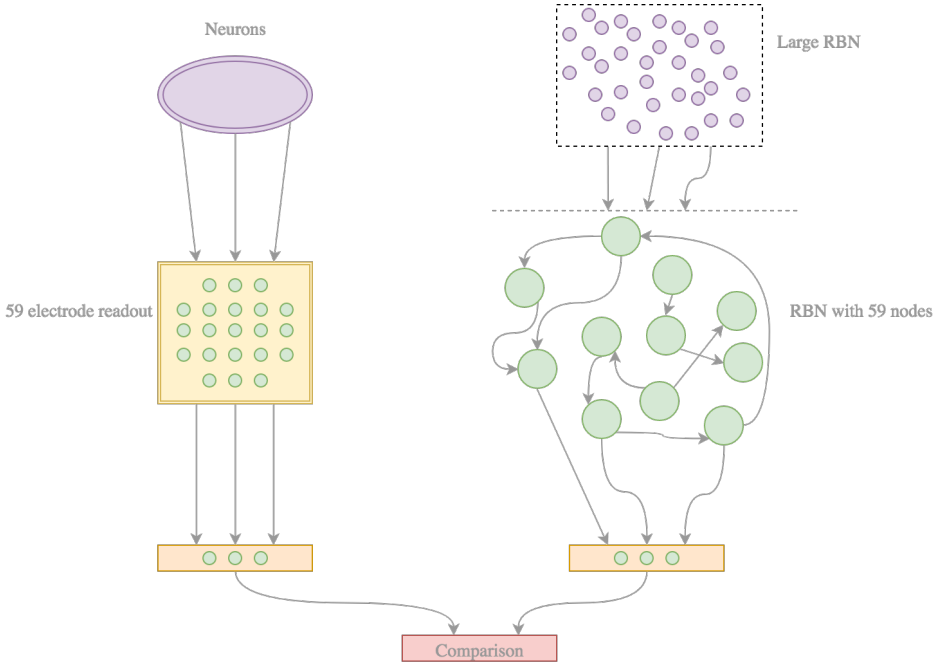

Figure 3.6: Overview of the comparison process.
Left: The neuron culture outputs data to the electrodes, the data gets processed and turned into bit string for comparison.
Right: The RBNs generated represents virtual nodes from a larger system, mimicking the electrodes and outputs bit string for comparison.

Chapter 4

Experiments

4.1 Complexity Evolution of Spatially-Constrained RBNs

4.1.1 Description

For this experiment 1000 RBNs are generated for each of the 15 time steps, mimicking the range of days the neuron cultures were recorded. A quick summary of the RBN is that the nodes are placed in a grid in the same positions as the electrodes in the MEA2100-60-system from MultiChannel Systems[13]. The rest of the setup for the RBNs can be reviewed in table 3.3. The *distant connect* probabilities follows the normal curve (figure 3.3) with $\mu = 0$ and a σ value that increases by each time step. Four different σ ranges were tested with a linear increase, where all starts at 0.0 and have a maximum value of 3, 4, 5 and 6 respectively. Note that the start value of the interval is a small value close to 0 and not absolute 0, this is to avoid zero division in the normal distribution formula. For instance, with a linear increase of σ and a maximum value of 3.0, the value for each time step is $[0.001, 0.214, 0.428, 0.642\ , ..., 3.0]$. This means that the day labelled 0 will have the normal probability distribution with μ = 0 and σ = 0.001, day 1 : σ = 0.214 and so on. The change in the probability distribution will change the *distant connect* probabilities, which will affect the chance each node have to connect to other nodes further away, where higher σ value will make it more likely for these distant connections to happen. All the tested ranges and their respectively probabilities can be reviewed in table 5.1, 5.2, 5.3 and 5.4 in the Appendix (chapter 5.2).

$$P(x) = \frac{1}{\sigma\sqrt{2\pi}} e^{-(x-\mu)^2/2\sigma^2}$$

Figure 4.1: The normal distribution function used to generate each probability value for each time step for the different configurations. μ = 0 and σ is in the range shown in table 4.1.

Max σ	**Range**
3	[0.0, 0.21429, 0.42857, 0.64286, 0.85714, 1.07143, 1.28571, 1.5, ... , 3.0]
4	[0.0, 0.28571, 0.57143, 0.85714, 1.14286, 1.42857, 1.71429, 2.0, ... , 4.0]
5	[0.0, 0.35714, 0.71429, 1.07143, 1.42857, 1.78571, 2.14286, 2.5, ... , 5.0]
6	[0.0, 0.42857, 0.85714, 1.28571, 1.71429, 2.14286, 2.57143, 3.0, ... , 6.0]

Table 4.1: The ranges of σ values used to produce normal distributions for *distant connect* probabilities for the RBNs generated at each time step. All ranges have a linear increase between 0 and the maximum σ value.

4.1.2 Result

The results of each of the 4 configurations are shown in the figure 4.2. Each of the plots in the figures are equally scaled, meaning that some data points are outside the scope. The ranges tested are : [0,3], [0,4], [0,5] and [0,6], where each of these intervals have 15 steps as shown in the plots. The *distant connect* probability of each step for each of the ranges can be reviewed in the tables: 5.1, 5.2, 5.3, 5.4 in the Appendix (chapter 5.2). Figure 4.5 shows a comparison between all the mean value graphs from the figure 4.2. Furthermore, all the data points from the runs are plotted, colour coded and scaled such that all data points are included, for a complete picture. However, note that the plots are done sequentially, such that the last configuration (red, $\sigma : [0, 6]$) will show more because it will cover the other coloured data points that were plotted before. For more visual comparison, one candidate RBN from time step 0, 5, 10 and 14 is shown in 4.3 and 4.4 for RBNs with σ range [0,3] and [0,6]. Lastly the spike count graph of the run with the σ range [0,3] is shown in figure 4.7, as a representation of how RBNs generally jumps between zero and one. Only one spike count graph is shown because all 4 configurations looks very similar.

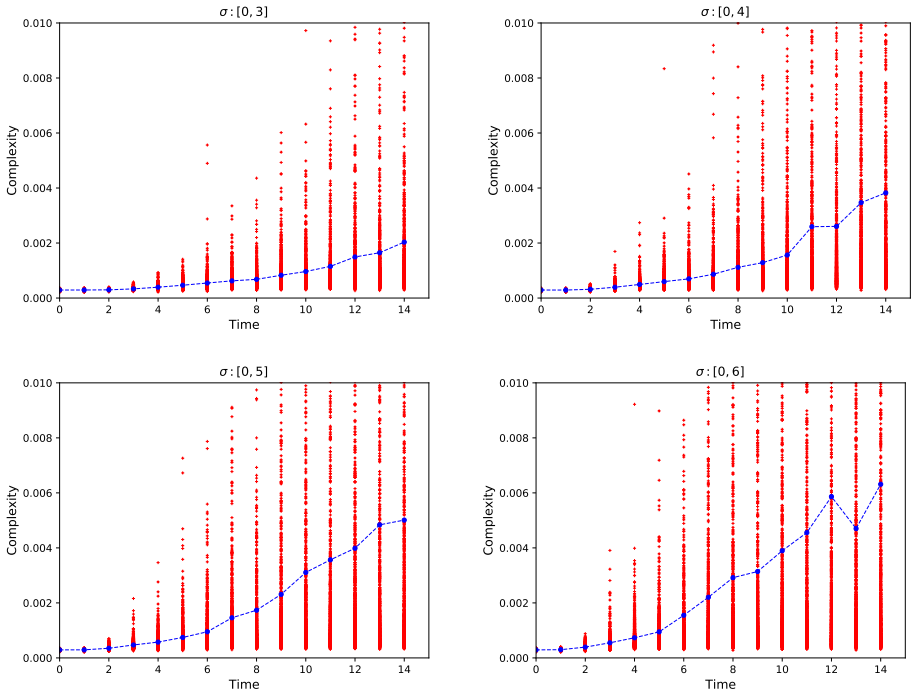

Figure 4.2:
Kolmogorov complexity evolution over 15 discrete time steps with linear increase of the *distant connect* parameter σ. Four different ranges of σ is shown. Each time step consists of 1000 individual RBNs generated with the probability distribution adjusted by σ.

4.1.3 Discussion

The result from the 4 different configurations shows a complexity increase across the board. As expected, the complexity is quite low in the first time steps, due to little to no connections to other nodes (illustration in 4.3 and 4.4, upper left). This means that most of the RBNs will stay frozen in one state (repeated point attractor) and the bit-patterns produced will stay repeated the same way, which makes it easy for the compression algorithm to compress. There seem to be a correlation between the *distant connect* probabilities and how complex the bit-patterns produced by the RBNs are. Since the amount of time steps are the same for all intervals tested (See table 4.1), the chance of connecting to more distant nodes will grow faster for those with greater maximum end point, due to a quicker transition to more flat and evenly distributed curve. The plots in figure 4.2 reflects these increases quite well. As the nodes connects to other nodes further away, the bit patterns gets overall more complex and the extreme values (high above the mean) seem to be more frequent. Figure 4.5, shows all the mean graphs in the same plot for comparison. Although the outliers exist for all configurations, the complexity will flatten out as the σ reaches a certain point if more time steps are included. This means that the all configurations will

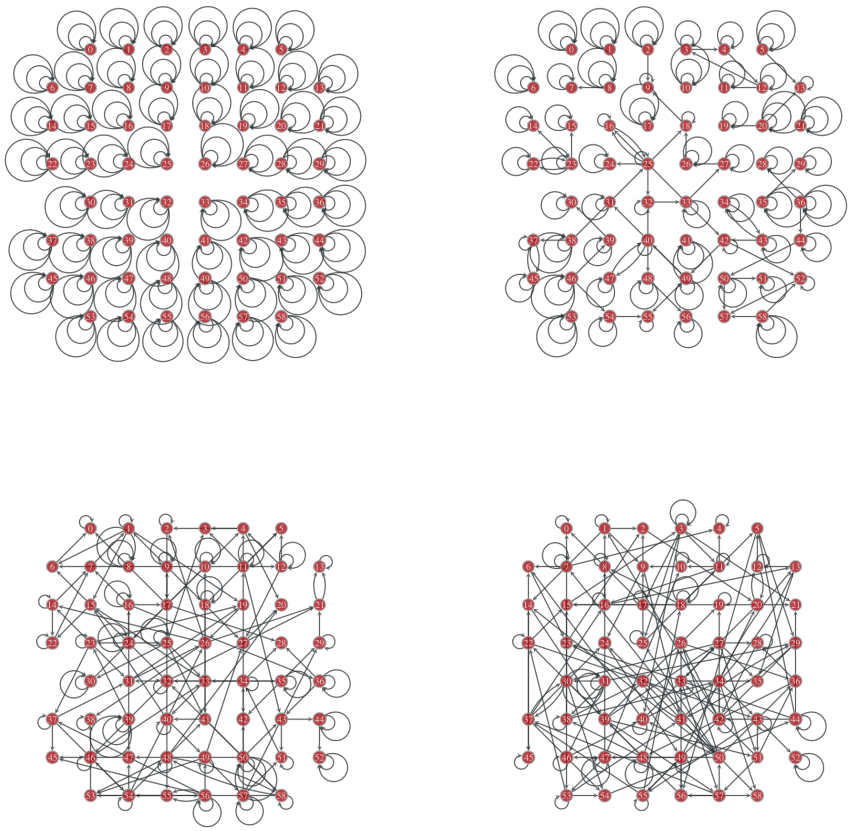

Figure 4.3: One candidate RBN from time step 0, 5, 10 and 14 with the σ : [0,3]. From upper left to lower right, the evolution of how connections changes as the nodes of the RBN are gradually allowed to connect to other nodes further and further away. Note: All RBNs are generated at random with *distant connect* probabilities of each respective σ values in the range [0,3], not the same network.

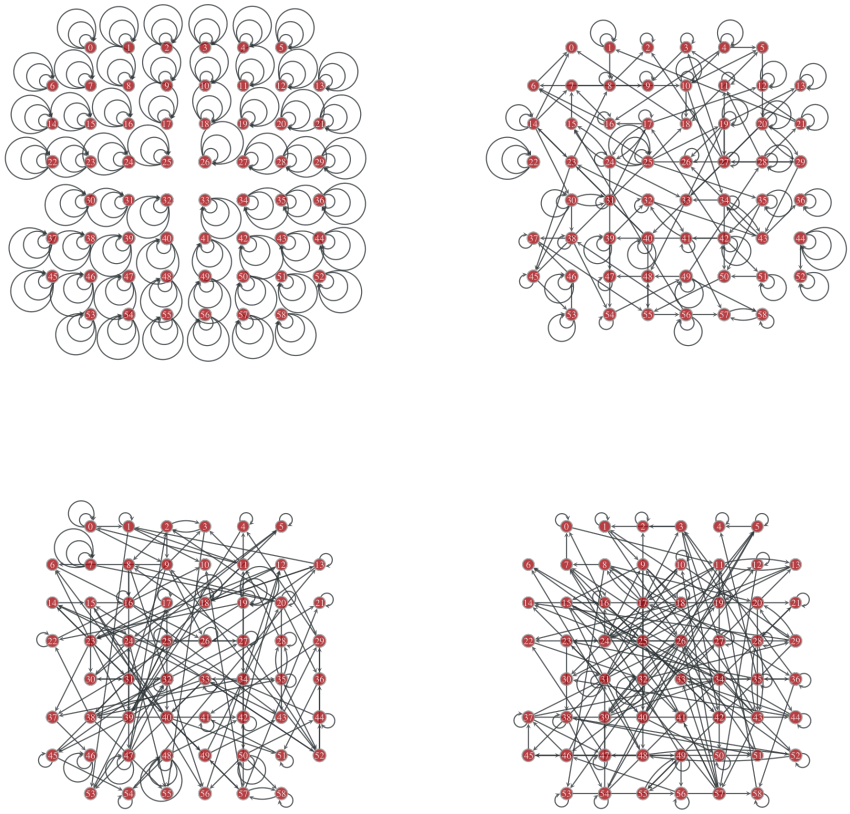

Figure 4.4: One candidate RBN from time step 0, 5, 10 and 14 with the σ : [0,6]. From upper left to lower right, the evolution of how connections changes as the nodes of the RBN are gradually allowed to connect to other nodes further and further away. Note: All RBNs are generated at random with *distant connect* probabilities of each respective σ values in the range [0,6], not the same network.

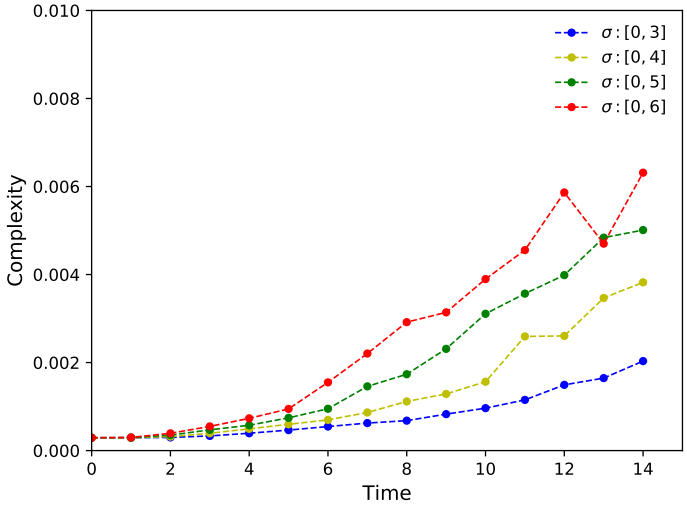

Figure 4.5: Mean values from fig 4.2 plotted against each other.

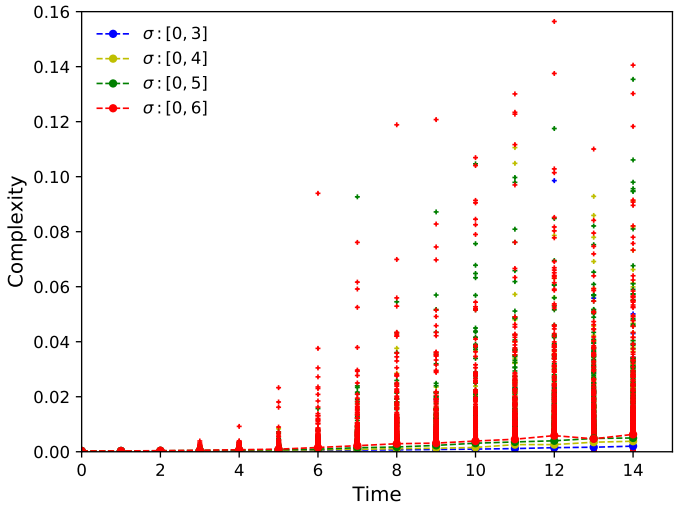

Figure 4.6: All plots from 4.2 together with the whole range of complexity values (not zoomed in).

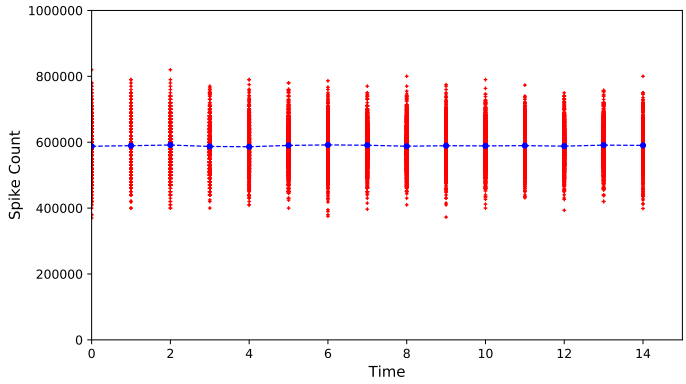

Figure 4.7: Spike count of the RBN configuration with the σ range [0,3].The maximum spikes that can occur per sample is $59 \times 20,000$ = 1,180,000.

reach a point where the chance of connecting to all nodes in the network will be the same. For the largest number of σ for these tests ($\sigma = 6$), the *distant connect* probabilities is quite evenly distributed with the values [0.13237, 0.12875, 0.12181, 0.11209, 0.10033, 0.08735, 0.07397, 0.06092, 0.18242] or normalised without the leftover probabilities (last element) [0.1619, 0.15748, 0.14899, 0.1371, 0.12271, 0.10684, 0.09047, 0.07451]. Giving a quite decent chance of connecting to nodes in all distances, 16.19% to the closest one (itself) and nodes furthest away 7.45% that is. The plots shows that, by tuning the growth function, the complexity of this particular RBN system can in indeed be controlled. By tuning the growth rate of σ, the ranges of complexity patterns can be restricted and used to design system behaviours that might resembles e.g. neurons in the MEA-chambers. Lastly the "spikes" of the RBNs were counted. As expected, all the configurations tested had a quite evenly distributed spiking numbers. This is due to RBNs and their ability to always deliver update for the next state(no loss of data). Once a RBN reaches an attractor, the data pattern produced will stay the same for the rest of the sample time, giving a consistent count. This also makes the spike count measurement less useful for comparison. Typical spike count plot for RBN configurations of these experiments is shown in figure 4.7.

Table 4.2: End point probabilities of the different configurations tested. The leftover values at the long tails are removed and the probabilities normalised to 1.

σ	**Probabilities**
3.0	[0.26314, 0.23571, 0.18912, 0.13593, 0.08751, 0.05047, 0.02607, 0.01206]
4.0	[0.20682, 0.19435, 0.17163, 0.14242, 0.11106, 0.08139, 0.05605, 0.03627]
5.0	[0.17803, 0.17107, 0.15796, 0.14016, 0.1195, 0.0979, 0.07708, 0.0583]
6.0	[0.1619, 0.15748, 0.14899, 0.1371, 0.12271, 0.10684, 0.09047, 0.07451]

4.2 Complexity Evolution of Neuron Cultures

4.2.1 Description

For this experiment the raw MEA data for each channel of the recordings were locally filtered with the threshold formulas:

$$Th_{low} = \bar{x} - (5 \times s)$$

$$Th_{high} = \bar{x} + (5 \times s)$$

The formulas turns recorded values below and above the threshold to 1, using $\bar{x}$ (sample mean) and s (sample standard deviation) for each channel respectively. This is a standard procedure used in the MEA-recording framework and also widely used as a so called amplitude thresholding technique[16]. Two measurements were used to look at the data patterns, where the first measures the complexity evolution (Kolmogorov complexity) and the second the firing intensity (spike count) of the data. Since it was quite time consuming to run analysis over the whole length of the data stream, the recordings from each individual day were sampled 1,000 times each. The data sample window was 20,000 (2 seconds) in length for each channel of the data stream. Furthermore, the data sample window was fixed in time, meaning that all channels were sampled at the same time interval for each sample.

4.2.2 Result

By observation through microscope, it was reported that the neurons seemed to have little to no activity across all the channels, due to how they formed clusters. Figure 4.8 shows the Kolmogorov complexity evolution of four different cultures over the course of 15 days. Red dots are complexity values outputted by the Bzip2 compression algorithm[15] for each sample of each day. Same test with spike counting is shown in figure 4.9, where the same samples used for compression are used. The cultures are labelled as the numbers 33, 34, 36 and 37 which was their numeration in the raw data set. Figure 4.10 summarises the mean value of both Kolmogorov complexity and spike count measurements of the data samples from the 4 cultures.

4.2.3 Discussion

When working with neuron cultures in-vitro, there are numerous factors that can affect the result of the recording. Environmental factors such as temperature, humidity gas(nitrogen, oxygen, CO_2 concentration etc.[7], but also the very nature of neurons and how they grow is crucial to obtain good readout from the interfacing system. As mentioned earlier in this thesis, a study conducted by DeMarse et. al[19] reported that cultured neurons often matured 18-25 days after they are placed in the incubation chambers. In the case of neuron cultures used for this thesis, the neurons were observed to form some clusters early on, but did also loosen up a few days after. Viewing the result of the spike counting plots in figure 4.9, the cultures 33 and 37 seem to have a wider range of spiking activity compared

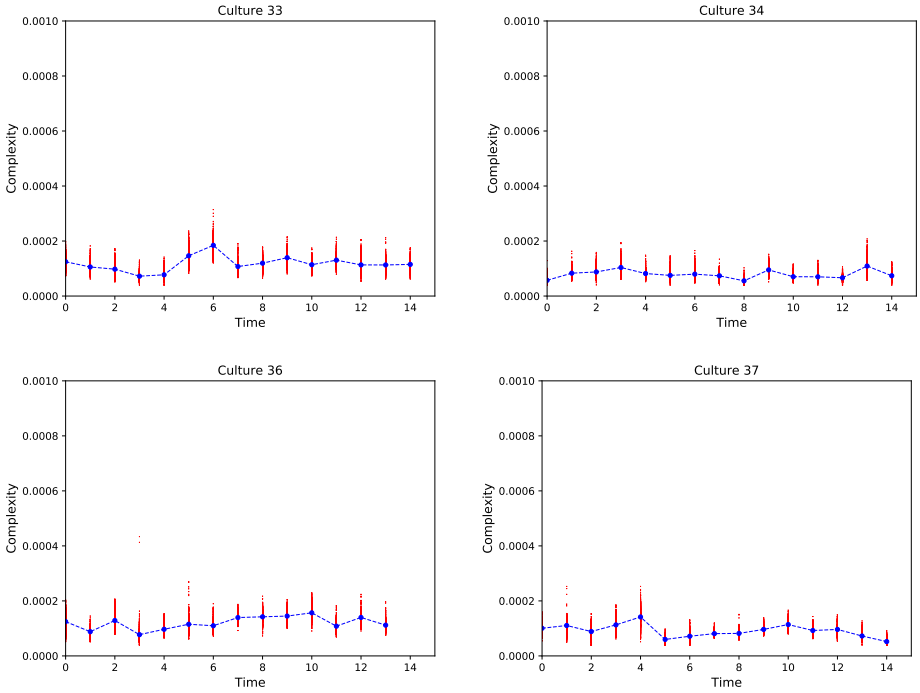

Figure 4.8:
Kolmogorov complexity for the neuron cultures labelled 33, 34, 36 and 37. The data stream from each day is sampled 1000 times, with a data sample window of 20, 000 in length. The start time for each sample is picked at random and fixed across all 59 channels.

to the other, an indication that it might have been more neurons close to the electrode. Furthermore the samples of 20,000 data points in length or 2 seconds of the recordings were sampled at random to try to capture potential spontaneous burst activity. This kind of activity have been reported to occur every 5-15 seconds, typically 100-1000 ms in duration in[19]. However, since all the cultures died out shortly after seeding, none of them reached the range of days where they could potentially have matured, 18-25 days that is. Another factor worth mention is that the channels are complexity measured and spike counted all together as a whole. With little activity across the board, potential channels with more activity might get drowned by the low activity captured by the rest of the electrodes. However, the spike count plots serves as a good indicator that the cultures overall had low activity. With 59 channels and 20,000 data points per channel, a range of spikes between 0 and 250 is considerably low compared to the total length of each sample ($59 \times 20,000$). Looking at earlier recordings of "successful" cultures, the complexity tend to increase over time after the cultures have matured. The leap towards more complex patterns and when it happens is still unknown. Figure 4.11 shows an example of how complexity may change over time, although the time interval is over a year, the evolution of complexity serves as a good pin point of what can be expected if the cultures had grown on the electrodes.

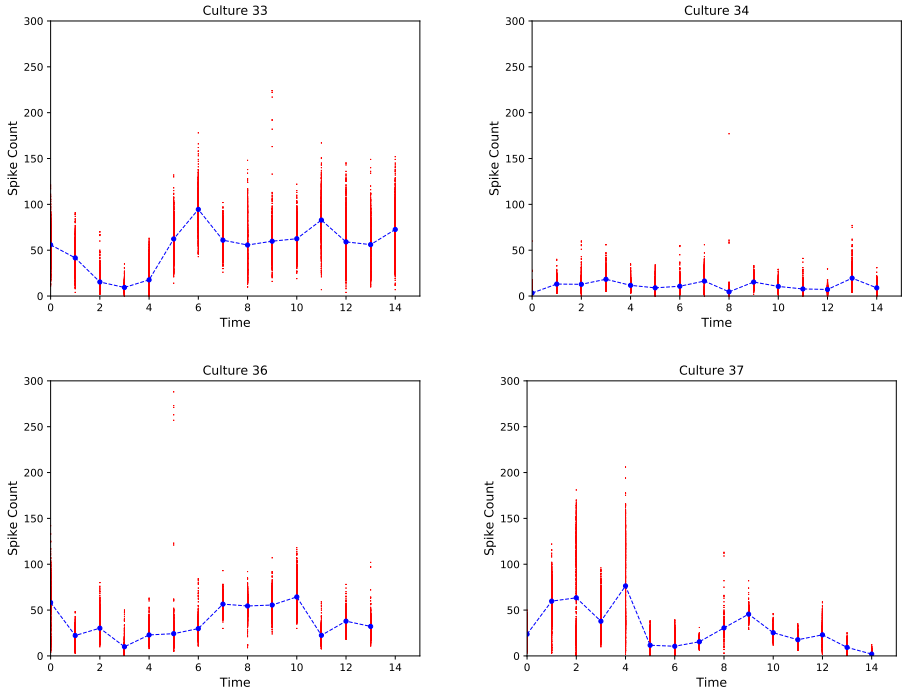

Figure 4.9:
Spike count for the neuron cultures labelled 33, 34, 36 and 37. The sample set of data is the same as the ones used in figure 4.8. Data stream from each day is sampled 1000 times, with a data sample window of 20,000 in length for each channel. The start time for each sample is picked at random and fixed across all 59 channels. Note: last day of culture 36 is missing due to technical problems with the recordings.

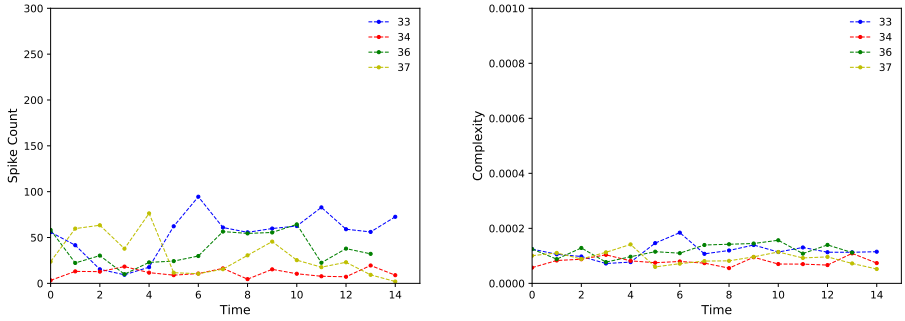

Figure 4.10:
Mean value of spike count and Kolmogorov complexity from the figures 4.8 and 4.9.

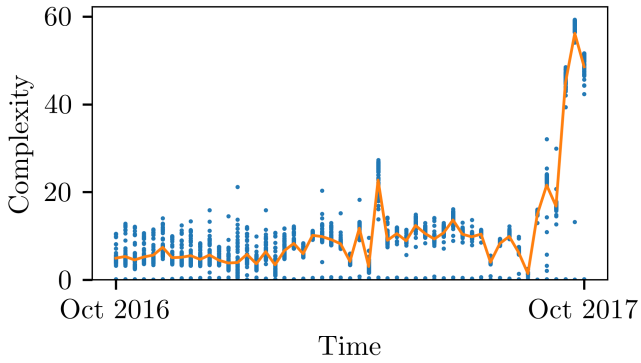

Figure 4.11: Approximated Kolmogorov complexity of the firing patterns over a one year period.[14] Note scaling difference between this and the plots from the experiments of this thesis.

4.3 Complexity Comparison Between Neuron Spiking- and RBN Patterns

4.3.1 Discussion

Since the neuron cultures cultivated for this task was unsuccessful in that none of them survived or reached the point where they matured, their complexity measures were also not a good representation of the developmental process. The complexity measurement of the neuron cultures were very similar and their order of magnitude is far below the RBN's. This is due to low activity from the neurons and that most of them did loosen up their binding from the electrode shortly after the seeding process. The spikes captured is also more likely to be regular noise, but were turned into spikes by the algorithm, due to very little activity. The spike count from the samples shows that out of $59 \times 20,000$, the spike count rarely got past 200 spikes, a very little fraction of the total sample that is. Figure 4.11 shows a good example of how cultures might grow in complexity as time goes by. However, due to more in-frequent recording of the cultures and stimuli applied, they do not serve as good for this experiment as the ones seeded for this thesis.

Chapter 5

Conclusion

5.1 Conclusion

Experiments have shown that RBNs when placed on a grid can have their bit-pattern complexity tuned, when restricting the chance each node have to connect to other distant nodes. The results shows that the *distant connect* probabilities indeed affect the network complexity and bit-patterns generated by the movement through state space. The bit-pattern complexity seem to increase as the chances of connecting to nodes further away increases. Tuning how the *distant connect* probabilities grows should in some degree help designing RBN systems that grows more like what have been observed in neuron cultures (e.g. 4.11). The data from neuron cultivation is often unpredictable both because of technological restriction and that the neurons them self not always are reliable. Data received for this thesis was not as representative as hoped for. Although data from earlier recordings were available, their recording were more infrequent and perturbation had been done to the cultures, making growth and change in structure more difficult to analyse. More data in the future will open up for better analysis with this model and potentially help fine-tuning it.

5.2 Future Work

The RBN configurations tested for the experiments of this thesis were restricted in that initial states, N, K and the *distant connect* probabilities were fixed. This helped in narrowing the immense search space down, giving a more controllable system. Since only four configurations of network were tested with one type of growth function(linear) of the *distant connect* probabilities, it would be interesting to see if we can control the system even more by adding on new parameters while testing new functions for *distant connect*. For instance by letting the number of in-degree K be varied instead of fixed for each node and letting the growth function be semi-exponential or logarithmic. However to truly test the grid-base RBN system, more representative data is needed. As more cultures are cultivated in the future, more data will be available for comparison and give the potential to further development of this grid-base RBN system.

Bibliography

[1] Derrida, B., and Pomeau, Y., 1986. Random Networks of Automata: A simple annealed approximation. Europhys. Lett., 1(2) 45 – 49.

[2] Fabrice O. Morin,Yuzuru Takamura, and Eiichi Tamiya, 2005. Investigating neuronal activity with planar microelectrode arrays: achievements and new perspectives. Journal of bioscience and bioengineering, 100(2), 131 – 143.

[3] Gershenson, C., 2004. "Introduction to random boolean networks". arXiv preprint nlin/0408006.

[4] H. C. Barron, T. P. Vogels, U. E. Emir, T. R. Makin, J. O'Shea, S. Clare, S. Jbabdi, R. J. Dolan, and T. E J Behrens, 2015. Unmasking Latent Inhibitory Connections in Human Cortex to Reveal Dormant Cortical Memories. Neuron, 1 – 13.

[5] Herculano-Houzel, S., 2009. The human brain in numbers: A linearly scaled-up primate brain. Frontiers in Human Neuroscience.;3(31).

[6] Kauffman, S. A., 1969. "Metabolic stability and epigenesis in randomly constructed genetic nets". Journal of theoretical biology 22.3, 437 – 467.

[7] Knudsen August Martinius, 2016. NTNU Cyborg: A study into embodying Neuronal Cultures through Robotic Systems. NTNU Open.

[8] Langton, C. G., 1991. "COMPUTATION AT THE EDGE OF CHAOS: PHASE TRANSITIONS AND EMERGENT COMPUTATION". Space 3.5 (), 27 – 28.

[9] Li, Ming; Paul Vitanyi, 1997. An Introduction to Kolmogorov Complexity and Its Applications (2nd ed.). Springer. Neuron, 90.

[10] Marco Ballini et al., 2014. "A 1024-channel CMOS microelectrode array with 26,400 electrodes for recording and stimulation of electrogenic cells in vitro.". IEEE Journal of Solid-State Circuits, 49(11):2705 – 2719.

[11] Martin Gardner, 1970. The fantastic combinations of John Conway's new solitaire game "life". Scientific American 223, 120 – 123.

[12] Millet, L. J., and Gillette, M. U., 2012. Over a Century of Neuron Culture: From the Hanging Drop to Microfluidic Devices. The Yale Journal of Biology and Medicine 85(4), 501–521.

[13] MultiChannel Systems, Website. Mea2100. https://www.multichannelsystems.com/products/mea2100-systems, accessed: 2018-05-24.

[14] NFR Project SOCRATES, 2017. Phase 1. https://www.ntnu.edu/socrates/phase1, accessed: 2018-05-15.

[15] Python Docs, Website. bz2. https://docs.python.org/2.7/library/bz2.html, accessed: 2018-05-26.

[16] Quiroga, R. Q., 2007. Spike sorting. Scholarpedia 2 (12), 3583, revision #137442.

[17] Smith, K., 10 2015. Surprise 'mystery' neurons found in male worms. Nature.

[18] Stephen Wolfram, 1984. Cellular automata as models of complexity. Nature volume 311, 419 – 424.

[19] T. DeMarse, A. Cadotte, P. Douglas, P. He, and V. Trinh, 2004. Computation within cultured neural networks. In Annual International Conference of the IEEE Engineering in Medicine and Biology, volume 7, 5340 – 5343.

[20] Thomas, C., Springer, P., Loeb, G., Berwald-Netter, Y.,and Okun, L., 1972. A miniature microelectrode array to monitor the bioelectric activity of cultured cells. Exp. Cell Res., 74, 61 – 66.

Appendix

axolGEM iPSC-Derived Neural Stem Cells LRRK2 G2019S HOM

Description

Human iPSC-Derived Neural Stem Cells that have been genetically edited using CRISPR-Cas9 technology to introduce the G2019S mutation (GGC>AGC) in the LRRK2 gene. This line is homozygous for the G2019S mutation so both alleles contain the mutation. The G2019S mutation in LRRK2 has been implicated in autosomal-dominant familial Parkinson's disease with late onset (Fonzo et al., 2006, Thaler et al., 2009). The G2019S mutation increases the kinase activity of LRRK2 causing increased autophosphorylation and substrate phosphorylation that may affect neuronal cell health in Parkinson's disease patients (West et al., 2005).
More information about the stem cells may be found at:
`https://www.axolbio.com/page/neural-stem-cells-cerebral-cortex`

5.2.1 Distant Connect Probabilities

Table 5.1: Distant connect probabilities at each time step with σ in range [0,3], where the first index corresponds to the chance of connecting to itself. The last index is the leftover probabilities in the long tails on both sides of the curve.

σ	**Probabilities**
0.0	[1.0, 0.0, 0.0, 0.0, 0.0, 0.0, 0.0, 0.0, 0.0]
0.21429	[1.0, 0.0, 0.0, 0.0, 0.0, 0.0, 0.0, 0.0, 0.0]
0.42857	[0.98037, 0.01963, 0.0, 0.0, 0.0, 0.0, 0.0, 0.0, 0.0]
0.64286	[0.88018, 0.11795, 0.00186, 0.0, 0.0, 0.0, 0.0, 0.0, 0.0]
0.85714	[0.75666, 0.22371, 0.01917, 0.00046, 0.0, 0.0, 0.0, 0.0, 0.0]
1.07143	[0.64935, 0.2887, 0.05684, 0.00492, 0.00019, 0.0, 0.0, 0.0, 0.0]
1.28571	[0.5633, 0.31689, 0.10018, 0.01777, 0.00176, 0.0001, 0.0, 0.0, 0.0]
1.5	[0.49501, 0.32256, 0.13692, 0.03784, 0.0068, 0.00079, 6e-05, 0.0, 0.0]
1.71429	[0.44033, 0.31632, 0.16323, 0.06049, 0.01609, 0.00307, 0.00042, 4e-05, 0.0]
1.92857	[0.3959, 0.30438, 0.1799, 0.08174, 0.02855, 0.00766, 0.00158, 0.00025, 3e-05]
2.14286	[0.35926, 0.29009, 0.18913, 0.09957, 0.04232, 0.01452, 0.00402, 0.0009, 0.00019]
2.35714	[0.32861, 0.27522, 0.19305, 0.11341, 0.0558, 0.02299, 0.00793, 0.00229, 0.00069]
2.57143	[0.30264, 0.26066, 0.19336, 0.12353, 0.06797, 0.03221, 0.01315, 0.00462, 0.00186]
2.78571	[0.28039, 0.24683, 0.19127, 0.13048, 0.07836, 0.04142, 0.01928, 0.0079, 0.00408]
3.0	[0.26112, 0.2339, 0.18767, 0.13489, 0.08684, 0.05008, 0.02587, 0.01197, 0.00766]

Table 5.2: Distant connect probabilities at each time step with σ in range [0,4], where the first index corresponds to the chance of connecting to itself. The last index is the leftover probabilities in the long tails on both sides of the curve.

σ	**Probabilities**
0.0	[1.0, 0.0, 0.0, 0.0, 0.0, 0.0, 0.0, 0.0, 0.0]
0.28571	[0.99953, 0.00047, 0.0, 0.0, 0.0, 0.0, 0.0, 0.0, 0.0]
0.57143	[0.91988, 0.07965, 0.00047, 0.0, 0.0, 0.0, 0.0, 0.0, 0.0]
0.85714	[0.75666, 0.22371, 0.01917, 0.00046, 0.0, 0.0, 0.0, 0.0, 0.0]
1.14286	[0.61842, 0.30146, 0.07145, 0.0082, 0.00045, 1e-05, 0.0, 0.0, 0.0]
1.42857	[0.51607, 0.32241, 0.12578, 0.03062, 0.00464, 0.00044, 3e-05, 0.0, 0.0]
1.71429	[0.44033, 0.31632, 0.16323, 0.06049, 0.01609, 0.00307, 0.00042, 4e-05, 0.0]
2.0	[0.38292, 0.29976, 0.1837, 0.08811, 0.03308, 0.00972, 0.00223, 0.0004, 6e-05]
2.28571	[0.33825, 0.28018, 0.19222, 0.10923, 0.05141, 0.02004, 0.00647, 0.00173, 0.00047]
2.57143	[0.30264, 0.26066, 0.19336, 0.12353, 0.06797, 0.03221, 0.01315, 0.00462, 0.00186]
2.85714	[0.27366, 0.24241, 0.19021, 0.1322, 0.08139, 0.04439, 0.02144, 0.00918, 0.00511]
3.14286	[0.24965, 0.22581, 0.18473, 0.13669, 0.09148, 0.05538, 0.03032, 0.01502, 0.01091]
3.42857	[0.22946, 0.21087, 0.1781, 0.13823, 0.0986, 0.06463, 0.03893, 0.02155, 0.01963]
3.71429	[0.21225, 0.19749, 0.17099, 0.13775, 0.10326, 0.07203, 0.04675, 0.02823, 0.03125]
4.0	[0.19741, 0.18551, 0.16382, 0.13594, 0.10601, 0.07769, 0.0535, 0.03462, 0.0455]

Table 5.3: Distant connect probabilities at each time step with σ in range [0,5], where the first index corresponds to the chance of connecting to itself. The last index is the leftover probabilities in the long tails on both sides of the curve.

σ	**Probabilities**
0.0	[1.0, 0.0, 0.0, 0.0, 0.0, 0.0, 0.0, 0.0, 0.0]
0.35714	[0.99489, 0.00511, 0.0, 0.0, 0.0, 0.0, 0.0, 0.0, 0.0]
0.71429	[0.83848, 0.15641, 0.00508, 3e-05, 0.0, 0.0, 0.0, 0.0, 0.0]
1.07143	[0.64935, 0.2887, 0.05684, 0.00492, 0.00019, 0.0, 0.0, 0.0, 0.0]
1.42857	[0.51607, 0.32241, 0.12578, 0.03062, 0.00464, 0.00044, 3e-05, 0.0, 0.0]
1.78571	[0.42452, 0.31277, 0.16976, 0.06787, 0.01998, 0.00433, 0.00069, 8e-05, 1e-05]
2.14286	[0.35926, 0.29009, 0.18913, 0.09957, 0.04232, 0.01452, 0.00402, 0.0009, 0.00019]
2.5	[0.31084, 0.26545, 0.19357, 0.12054, 0.0641, 0.02911, 0.01128, 0.00374, 0.00137]
2.85714	[0.27366, 0.24241, 0.19021, 0.1322, 0.08139, 0.04439, 0.02144, 0.00918, 0.00511]
3.21429	[0.24428, 0.22192, 0.18315, 0.13731, 0.09352, 0.05787, 0.03253, 0.01661, 0.01281]
3.57143	[0.22052, 0.204, 0.17457, 0.13819, 0.1012, 0.06856, 0.04296, 0.0249, 0.02509]
3.92857	[0.20093, 0.18839, 0.1656, 0.13649, 0.10548, 0.07642, 0.05191, 0.03307, 0.04171]
4.28571	[0.1845, 0.17476, 0.15681, 0.13328, 0.1073, 0.08183, 0.05911, 0.04045, 0.06195]
4.64286	[0.17053, 0.16283, 0.14846, 0.12924, 0.10743, 0.08526, 0.06462, 0.04676, 0.08487]
5.0	[0.15852, 0.15232, 0.14065, 0.1248, 0.1064, 0.08717, 0.06863, 0.05191, 0.1096]

Table 5.4: Distant connect probabilities at each time step with σ in range [0,6], where the first index corresponds to the chance of connecting to itself. The last index is the leftover probabilities in the long tails on both sides of the curve.

σ	**Probabilities**
0.0	[1.0, 0.0, 0.0, 0.0, 0.0, 0.0, 0.0, 0.0, 0.0]
0.42857	[0.98037, 0.01963, 0.0, 0.0, 0.0, 0.0, 0.0, 0.0, 0.0]
0.85714	[0.75666, 0.22371, 0.01917, 0.00046, 0.0, 0.0, 0.0, 0.0, 0.0]
1.28571	[0.5633, 0.31689, 0.10018, 0.01777, 0.00176, 0.0001, 0.0, 0.0, 0.0]
1.71429	[0.44033, 0.31632, 0.16323, 0.06049, 0.01609, 0.00307, 0.00042, 4e-05, 0.0]
2.14286	[0.35926, 0.29009, 0.18913, 0.09957, 0.04232, 0.01452, 0.00402, 0.0009, 0.00019]
2.57143	[0.30264, 0.26066, 0.19336, 0.12353, 0.06797, 0.03221, 0.01315, 0.00462, 0.00186]
3.0	[0.26112, 0.2339, 0.18767, 0.13489, 0.08684, 0.05008, 0.02587, 0.01197, 0.00766]
3.42857	[0.22946, 0.21087, 0.1781, 0.13823, 0.0986, 0.06463, 0.03893, 0.02155, 0.01963]
3.85714	[0.20456, 0.19134, 0.1674, 0.13698, 0.10485, 0.07506, 0.05026, 0.03148, 0.03807]
4.28571	[0.1845, 0.17476, 0.15681, 0.13328, 0.1073, 0.08183, 0.05911, 0.04045, 0.06195]
4.71429	[0.16799, 0.16062, 0.14685, 0.12837, 0.1073, 0.08575, 0.06553, 0.04788, 0.0897]
5.14286	[0.15417, 0.14847, 0.13769, 0.12297, 0.10576, 0.0876, 0.06987, 0.05366, 0.11981]
5.57143	[0.14244, 0.13794, 0.12936, 0.11747, 0.1033, 0.08797, 0.07255, 0.05794, 0.15103]
6.0	[0.13237, 0.12875, 0.12181, 0.11209, 0.10033, 0.08735, 0.07397, 0.06092, 0.18242]